Emitter degradation in quantum dot intermediate band solar cells

A. Martí,[a] N. López, E. Antolín, E. Cánovas, and A. Luque
Instituto de Energía Solar, E.T.S.I. Telecomunicación, Universidad Politécnica de Madrid, Ciudad Universitaria s/n, Madrid 28040, Spain

C. R. Stanley, C. D. Farmer, and P. Díaz
Department of Electronics and Electrical Engineering, University of Glasgow, Oakfield Avenue, Glasgow G12 8LT, United Kingdom

(Received 15 September 2006; accepted 16 May 2007; published online 7 June 2007)

The characteristics of intermediate band solar cells containing 10, 20, and 50 InAs quantum dot (QD) layers embedded in otherwise "standard" (Al,Ga)As solar cell structures have been compared. The short-circuit current densities of the cells decreased and the quantum efficiencies of the devices showed a concomitant reduction in the minority carrier lifetime in the *p* emitters with increasing number of QD layers. Dislocations threading up from the QDs toward the surface of the cells, and revealed by bright field scanning transmission electron microscopy, are the most likely cause of the deterioration in the electrical performance of the cells. © *2007 American Institute of Physics*. [DOI: 10.1063/1.2747195]

The intermediate band solar cell (IBSC) is a photovoltaic concept designed to give a performance exceeding that of single gap solar cells.[1,2] The basic principles behind its operation rely on synthesizing a semiconductor material with an electronic band located within the band gap [Fig. 1(a)]. This band must be half-filled with electrons to allow the absorption of below band-gap energy photons and their conversion into photocurrent without voltage degradation. In addition, carrier recombination between bands should be much slower than the relaxation within the bands so that the carrier concentration of each band is described by its own quasi-Fermi level. A discussion of how it might be possible to prevent the intermediate energy centers from becoming nonradiative recombination ones, which would degrade rather than enhance the performance of the cell, can be found in Ref. 3.

Quantum dots (QDs) have been proposed as a way of both implementing the intermediate band concept[4,5] and studying its principles of operation. In this approach, the intermediate band would arise from the confined states of the electrons in the QDs [Fig. 1(a)]. Quantum dot intermediate band solar cells (QD-IBSCs) have been manufactured and tested in the past,[6–8] based on InAs and GaAs for the dot and barrier materials respectively. The QD-IBSC structures [see Fig. 1(b)] were grown on 3 in. diameter Si-GaAs(100) substrates in a solid source molecular beam epitaxy (MBE) system using As_2. The group III fluxes were calibrated by reflection high-energy electron diffraction intensity oscillations, and in the case of In the flux was set to give a growth rate of ~0.032 (ML/s) as measured on an InAs calibration sample. The QDs were formed under the Stransky-Krastanov growth mode[9] by depositing ~2.7 ML of InAs, either with or without a direct As_2 flux. A growth interrupt during the deposition of the GaAs capping layer was used to introduce Si δ doping with an areal density to match the QD density. All the layers in the QD stacks were grown at ~460 °C, while the (Al,Ga)As layers of the p^+ and n^+ emitters, and the *n* base were grown at 580–600 °C. The devices confirmed that the production of photocurrent from the absorption of below band-gap energy photons is possible and that the population of electrons in each band is best described by its own quasi-Fermi level, two of the basic principles underlying IBSC operation.

The experiments have also shown, however, that the contribution from the QDs to the photocurrent of the cell is small. This was attributed to the fact that devices with only ten layers (×10) of QDs were used in the experiments, implying an insufficient volume of material for significant sub-band-gap photon absorption. In order to solve this problem, QD-IBSCs with an increased number of QD layers (×20 and ×50) have been designed and manufactured. The basic common structure of these cells, shown in Fig. 1(b), consists of a *p*-emitter and *n* base sandwiching the region that contains the QDs.

The current-voltage characteristics of the devices were measured under one sun illumination (100 mW cm^{-2} Global spectrum[10]) with the results shown in Fig. 2. As can be seen, the performance of the devices worsens when the number of quantum dot layers increases, contrary to our initial expecta-

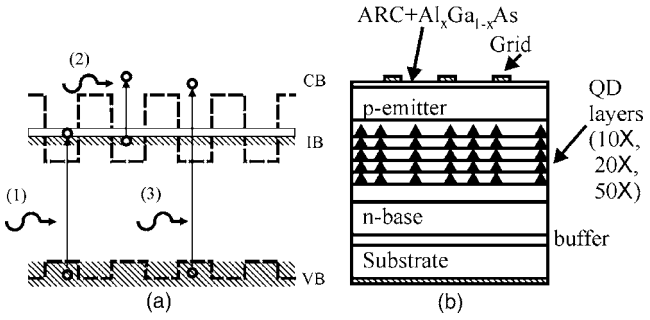

FIG. 1. (a) Schematic diagram showing the intermediate band concept. Photons (1) and (2) pump electrons from the valence band (VB) to the intermediate band (IB) and from the IB to the conduction band (CB), respectively. These two photons create one net electron-hole pair that adds to the ones generated directly by photons such as (3) with enough energy to pump an electron directly from the VB to the CB. Dashed lines represent the CB and VB potential wells when the cell is implemented with quantum dots. (b) Simplified internal structure of the intermediate band solar cells implemented with quantum dots and used in these experiments.

[a]Electronic mail: amarti@etsit.upm.es

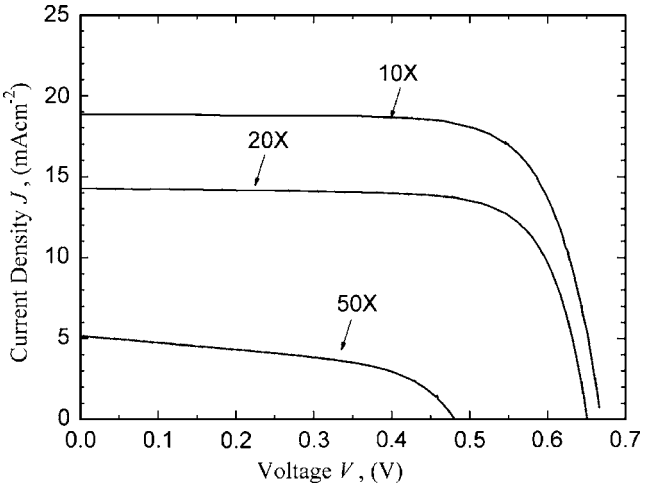

FIG. 2. Current-voltage characteristics of quantum dot intermediate band solar cells consisting of ×10, ×20, and ×50 layers of quantum dots (100 mW cm^{-2} AM1.5 Global spectrum). Current density is referred to the cell area excluding the bus bar.

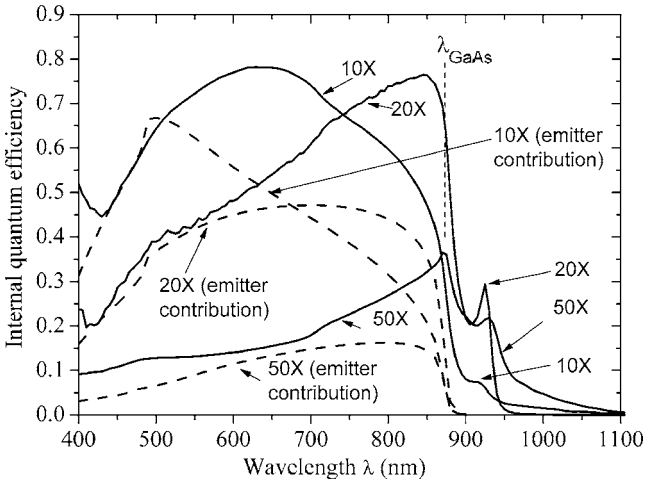

FIG. 3. Internal quantum efficiency corresponding to quantum dot intermediate band solar cells with ×10, ×20, and ×50 layers of quantum dot (connected lines). The dashed lines correspond to the estimated contribution from the p emitter of the cells. λ_{GaAs} is the GaAs gap wavelength and is shown for reference.

tion. Moreover, this deterioration is mostly associated with a degradation of their short-circuit current. An analysis of the quantum efficiency (QE) of the devices (see Fig. 3) provides insight into the cause of this degradation.

The internal QE of the devices was determined from a direct measurement of their external QE by discounting the shadowing factor, and the residual surface reflectivity arising from the combined effects of the antireflective coating (ARC) and the AlGaAs window layer. The latter was calculated using standard models[11] based on the estimated values of the thickness and refraction index of the layers involved in the structures (see Table I). Although it is not the main topic of the discussion of this letter, note the extended QE response provided by the quantum dot layers for wavelengths exceeding that of the GaAs gap (λ_{GaAs}). Moreover, note also in Fig. 3 that the contribution to the photocurrent from the quantum dots increases as the number of layers increases from ×10 to ×20. No further improvement is observed when going to the ×50 case due probably to the same general degradation phenomenon that is discussed next.

Figure 3 also shows the contribution from the p emitter to the internal QE of the cells, as calculated using Hovel's[12] model with the parameters summarized in Table I. The results confirm that the degradation in the short-circuit current (J_{sc}) is due largely to a reduction in the contribution from the p emitter. A similar degradation of J_{sc} in multiple InGaAs–GaAs QD layers grown by metal-organic chemical vapor deposition has been attributed by Norman *et al.*[13] to the presence of Si δ doping, introduced between each layer of QDs to half-fill the intermediate band with electrons. We have no evidence to link the degradation to Si δ doping in our MBE grown structures.

It must be pointed out that the values of the parameters given in Table I are best estimates. Other combinations can generate similar shapes for the quantum efficiency curves, but all are consistent with degradation of the p-emitter response, as shown in Fig. 4. The measured quantum efficiency curve corresponding to the the ×20 case is also shown for reference. These results suggest that incrementing the number of layers causes the appearance of an increased number of strain-induced dislocations that propagate and accumulate toward the emitter as the growth proceeds.

Bright field scanning transmission electron microscopy (STEM) images of the ×10 and ×50 samples are shown in Fig. 5. The STEM image for the QD-IBSC with the ×10 QD stack, formed by depositing 2.7 ML of InAs with 10 nm thick GaAs spacer/capping layers [Fig. 5(a)], shows a vertical alignment of QDs in successive layers and the absence of dislocations, either within the QD stack or propagating up into the p-emitter region (top of image). In contrast, the STEM image of the QD-IBSC with ×50 QD layers [3.2 ML of InAs with 15 nm GaAs spacer/cap layers, Fig. 5(b)] shows a collapse of QD growth after ~34 layers. There appear to be approximately two QD layers missing and the final ~14 InAs/GaAs periods consist of InAs "wetting" layers rather than QDs. The presence of a high concentration of dislocations is evident, both within the QD layers and pen-

TABLE I. Data used in the modeling of the quantum efficiency of the cells and the contribution from the p emitter. τ_e, minority lifetime; S_e, surface recombination velocity at the $Al_xGa_{1-x}As$/emitter interface; L_e, minority carrier diffusion length; W_e, emitter thickness; n_r, averaged refraction index; t, ARC thickness; A, cell junction area; F_S, shadowing factor (including bus bar); and F_S^*, shadowing factor (excluding the bus bar).

		Emitter				$Al_xGa_{1-x}As$ window			ARC		Area		Shadowing factor	
Sample No.	Number of QD layers	τ_e (ns)	S_e (cm s^{-1})	L_e (μm)	W_e (μm)	x	n_r	t (nm)		n_r	t (nm)	A (mm^2)	F_S	F_S^*
A1681	×10	3.5	1.6×10^6	5.0	0.3	0.8	2.93	50	SiO_2	1.44	110	1.21	0.41	0.041
A1938	×20	2.0	1.8×10^6	2.7	0.9	0.8	2.93	50	SiN_x	1.90	75	0.77	0.46	0.124
A2058	×50	0.005	4.0×10^6	0.3	0.9	0.85	2.91	40	SiN_x	1.90	75	4.00	0.13	0.086

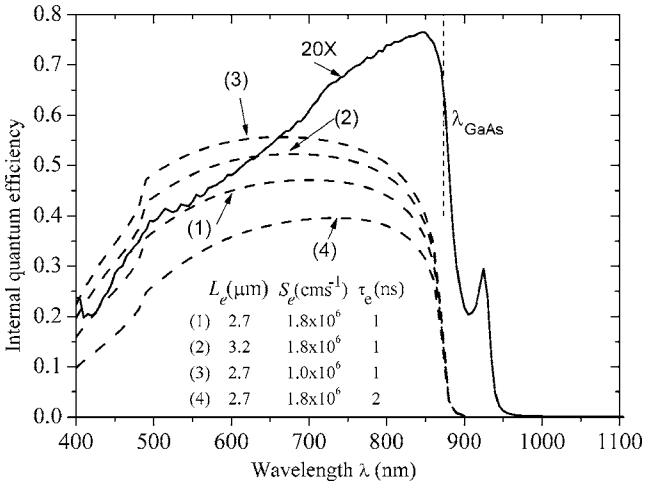

FIG. 4. Contribution from the *p* emitter to the internal quantum efficiency (dashed lines) for several values of the material parameters. The curve labeled (1) corresponds to our best estimate. The measured internal quantum efficiency of the ×20 cell is shown for reference (connected line).

etrating into the *p* emitter, leading to a significant nonradiative recombination and a reduction in the overall photocurrent delivered by the device.

In summary, we have investigated the performance of QD-IBSCs as the number of QD layers within the base region is increased. The QE response for wavelengths exceeding λ_{GaAs} is enhanced by the QD layers but overall, the cell performance degrades due to a reduction in the contribution to the photocurrent generated by the *p* emitter. This is explained by a decrease in the minority carrier lifetime, believed to be caused by strain-induced dislocations that propagate toward the *p* emitter from the QD region. The conclusion of this work is that practical QD-IBSCs, which require large numbers of QD layers for significant absorption of photons with energies less than the band gap of the host semiconductor, need to be grown with strain-relieving layers to avoid the formation of these dislocations. Such structures are feasible if InP substrates[14] are used.

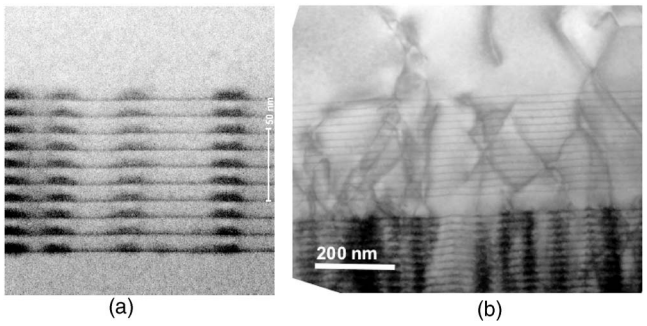

FIG. 5. (a) Bright field scanning transmission electron microscope (STEM) image through a stack of ×10 QD layers, formed by depositing 2.7 ML of InAs with 10 nm thick GaAs spacer/capping layers. The *p* emitter is above the QDs. (b) STEM image of a QD-IBSC with ×50 QD layers (3.2 ML of InAs with 15 nm GaAs spacer/cap layers). Note the collapse of QD growth after ~34 layers. There appear to be approximately two QD layers missing, before the final ~14 InAs/GaAs periods which consist of InAs "wetting" layers rather than QDs. The presence of a high concentration of dislocations in the *p*-emitter and elsewhere is evident.

This work has been supported by the European Commission within the project FULLSPECTUM (SES6-CT-2003-502620) and the projects NUMANCIA (S-0505/ENE/000310) funded by the Comunidad de Madrid and GENESIS-FV (CSD2006-0004) funded by the Spanish National Programme. One of the authors (E.C.) acknowledges a "Plan Nacional de Formación de Personal Investigador" research grant.

[1] A. Luque and A. Martí, Phys. Rev. Lett. **78**, 5014 (1997).
[2] A. Luque and A. Martí, Prog. Photovoltaics **9**, 73 (2001).
[3] A. Luque, A. Martí, E. Antolín, and C. Tablero, Physica B **382**, 320 (2006).
[4] A. Martí, L. Cuadra, and A. Luque, *Proceedings of the 28th IEEE Photovoltaics Specialists Conference* (IEEE, New York, 2000), pp. 940–943.
[5] A. Martí, L. Cuadra, and A. Luque, *Next Generation Photovoltaics: High Efficiency through Full Spectrum Utilization*, edited by A. Martí and A. Luque (Institute of Physics, Bristol, 2003), Chap. 7, pp. 140–162.
[6] A. Luque, A. Martí, N. López, E. Antolín, E. Cánovas, C. Stanley, C. Farmer, L. J. Caballero, L. Cuadra, and J. L. Balenzategui, Appl. Phys. Lett. **87**, 083505 (2005).
[7] A. Luque, A. Martí, C. R. Stanley, N. López, L. Cuadra, D. Zhou, and A. McKee, J. Appl. Phys. **96**, 903 (2004).
[8] A. Luque, A. Martí, N. López, E. Antolín, E. Cánovas, C. R. Stanley, C. Farmer, and P. Díaz, J. Appl. Phys. **99**, 094503 (2006).
[9] Y. Nakadata, Y. Sugiyama, and M. Sugawara, in *Self-assembled* InGaAs/GaAs *Quantum Dots*, edited by M. Sugawara (Academic, San Diego, 1999), Vol. 60, p. 119.
[10] R. Hulstrom, R. Bird, and C. Riordan, Sol. Cells **15**, 365 (1985).
[11] M. Born and E. Wolf, *Principles of Optics* (Pergamon, Oxford, 1975), 61.
[12] H. J. Hovel, *Solar Cells* (Academic, New York, 1975), 11, 15.
[13] A. G. Norman, M. C. Hanna, P. Dippo, D. H. Levi, R. C. Reedy, J. S. Ward, and M. M. Al-Jassim, *Proceedings of the 31st IEEE Photovoltaics Specialists Conference* (IEEE, New York, 2005), pp. 43–48.
[14] Y. Okada, N. Shiotsuka, H. Komiyama, K. Akahane, and N. Ohtani, *Proceedings of the 20th European Photovoltaic Solar Energy Conference* (WIP-Renewable Energies and ETA, Munich, 2005), pp. 51–54.